

Papers published in *Ocean Science Discussions* are under
open-access review for the journal *Ocean Science*

Indian Ocean subtropical mode water: its water characteristics and spatial distribution

T. Tsubouchi, T. Suga, and K. Hanawa

Department of Geophysics, Tohoku University, Sendai, Japan

Received: 20 March 2009 – Accepted: 12 April 2009 – Published: 21 April 2009

Correspondence to: T. Tsubouchi (tt2r07@noc.soton.ac.uk)

Published by Copernicus Publications on behalf of the European Geosciences Union.

723

Abstract

We examined Indian Ocean Subtropical Mode Water (IOSTMW) and described its characteristics using an isopycnally averaged three-dimensional hydrographic dataset. Through careful examination of the spatial distribution and water characteristics of the core in the layer of minimum vertical temperature gradient, we concluded that the IOSTMW exists as a robust structure in the western part of the Indian Ocean subtropical gyre in summer. The averaged IOSTMW properties during approximately 1960–2004 were $16.54 \pm 0.49^\circ\text{C}$, 35.51 ± 0.04 psu, and $26.0 \pm 0.1\sigma_\theta$. The IOSTMW distribution area was $27\text{--}38^\circ\text{S}$, $25\text{--}50^\circ\text{E}$.

1 Introduction

Subtropical Mode Water (STMW), which is characterized as a thermostad or pycnostad, is a remnant of the deepest winter mixed layer and is distributed in the western part of the subtropical gyre (Hanawa and Talley, 2001). Because the deepest mixed layer contains the memories of accumulated atmospheric forcing, such as winter cooling and wind stress, the STMW is thought to transmit these memories to the interior ocean below the winter mixed layer via the subduction mechanism (Marshall et al., 1993) and to the sea surface in the following winter through the reemergence mechanism (Hanawa and Sugimoto, 2004).

While several studies have provided fragmentary descriptions of the IOSTMW, they have been based solely on sectional observations along 32°S from November to December 1987 (Fine, 1993; Toole and Warren, 1993) or in March 2002 (McDonagh et al., 2005), or during the Agulhas Retroflexion Cruise (ARC) from November to December 1983 (Gordon et al., 1987; Olson et al., 1992). Sectional hydrographic data are not adequate for examining essential characteristics of STMW. As the essential characteristics, Mode Water produces the maximum inventory in a volumetric census of temperature and salinity over a relatively large geographical area throughout the warming

724

season. Therefore, it is still unclear whether the Indian Ocean STMW (IOSTMW) exists as a robust structure in the western part of the Indian Ocean subtropical gyre.

In this paper, we investigated the IOSTMW using an isopycnally averaged three-dimensional hydrographic dataset. We developed a basic description of the IOSTMW, such as water characteristics and spatial distribution. This procedure was not straight-forward due to the subsurface temperature stratification in this region at depths of 100 to 600 m. The temperature stratification is weaker than in other subtropical gyres, such as the North Pacific subtropical gyre (Fig. 1).

2 Data and method

We used the temperature and salinity data of the Indian Ocean HydroBase climatology (IOHB; Kobayashi and Suga, 2006). Because HydroBase was constructed by averaging the original profile data isopycnally, the reproducibility of density structure was generally better than for previous climatologies, especially around strong density fronts. Kobayashi and Suga (2006) showed that the IOHB has more realistic density stratification around the Antarctic Circumpolar Current (ACC) than does the World Ocean Atlas 2001 (Stephens et al., 2002; Boyer et al., 2002). The IOHB climatology was provided on a $1^\circ \times 1^\circ$ (latitude \times longitude) horizontal grid at standard depths from the surface to the bottom. The standard depth data were interpolated to 10-m vertical intervals using Akima's shape-preserving local spline method (Akima, 1970). The original monthly climatology data were averaged over January, February, and March to calculate summer mean climatology in the Southern Hemisphere.

We focused on the structure of the layer of minimum vertical temperature gradient (LMVTG) to investigate the remnant of the winter mixed layer using summer temperature data. The deep winter mixed layer is capped by the seasonal thermocline during the heating season. As a result, the LMVTG is generally formed between the seasonal and permanent thermoclines in summer. Hence, we were able to investigate the water originating from the winter mixed layer by detecting the LMVTG in the upper ocean

725

temperature structure.

The vertical temperature gradient was calculated from the temperature difference between adjacent grids below and above (their depth difference was 20 m). The LMVTG was defined as a minimum vertical temperature gradient layer thicker than 50 m. The core of the LMVTG was defined as the depth at which the absolute minimum of the vertical temperature gradient occurred for each profile. The core preserves the best record of the wintertime mixed layer conditions because it is likely to have suffered the least modification. Therefore, the water characteristics of the LMVTG core could be regarded as typical water characteristics of the LMVTG.

3 Water characteristics of the LMVTG

We selected two sub-regions of the western part of the subtropical gyre to characterize the vertical temperature gradient structure (Fig. 2): Region A ($33\text{--}38^\circ\text{S}$ and $27\text{--}35^\circ\text{E}$) and Region B ($33\text{--}38^\circ\text{S}$ and $40\text{--}48^\circ\text{E}$). In both sub-regions, each profile contained two LMVTG types: one colder than and one warmer than 15°C . The temperature range of each type was different in the two sub-regions. In Region A, the colder LMVTG appeared around $11.0\text{--}13.0^\circ\text{C}$, with a vertical temperature gradient as low as $1.1^\circ\text{C}/100\text{ m}$, and the warmer LMVTG appeared around $16.0\text{--}18.0^\circ\text{C}$, with a vertical temperature gradient lower than $1.4^\circ\text{C}/100\text{ m}$. In Region B, the colder LMVTG appeared around $12.0\text{--}14.5^\circ\text{C}$, with a vertical temperature gradient as low as $0.9^\circ\text{C}/100\text{ m}$, and the warmer LMVTG appeared around $15.5\text{--}17.0^\circ\text{C}$, with a vertical temperature gradient lower than $1.0^\circ\text{C}/100\text{ m}$. Previous studies (Gordon et al., 1987; Olson et al., 1992; McDonagh et al., 2005) have proposed the warmer LMVTG as a candidate for the IOSTMW. Here we examine the likelihood of this proposal.

We tested the existence of the IOSTMW by examining whether (a) this warmer LMVTG was distributed over a wide area in the western part of the subtropical gyre and (b) its water characteristics formed a modal class of temperature and salinity for the regional area census. These are the essential characteristics of STMW (Hanawa

726

and Talley, 2001).

Although we confirmed the existence of the warmer LMVTG in these sub-regions, we could not extract it objectively by applying any single threshold of vertical temperature gradient, as has been done in other cases. As shown in Fig. 2, we could not detect the warmer LMVTG in Region A by applying a threshold of $1.0^{\circ}\text{C}/100\text{ m}$, which was an appropriate threshold for detecting the warmer LMVTG in Region B. The vertical temperature gradient of the warmer LMVTG in Region A was higher than $1.0^{\circ}\text{C}/100\text{ m}$. Conversely, we could not detect the warmer LMVTG in Region B by applying a threshold of $1.4^{\circ}\text{C}/100\text{ m}$, which was an appropriate threshold for detecting the warmer LMVTG in Region A. The maximum vertical temperature gradient below the warmer LMVTG in Region B was lower than $1.4^{\circ}\text{C}/100\text{ m}$. This was different from the situation in other subtropical gyres. For example, we could detect the LMVTG corresponding to North Pacific STMW (NPSTMW; Masuzawa, 1969) in the western part of the North Pacific subtropical gyre reasonably by applying any single threshold of vertical temperature gradient from 1.0 to $1.8^{\circ}\text{C}/100\text{ m}$ (Fig. 1). It is important to note that this did not signify the vulnerability of the LMVTG; rather, the weak temperature stratification below the LMVTG presented a problem for detection. We were able to detect the warmer LMVTG in both sub-regions A and B reasonably by applying a single threshold of vertical temperature gradient from 1.4 to $2.0^{\circ}\text{C}/100\text{ m}$, if sufficient temperature stratification (greater than $2.0^{\circ}\text{C}/100\text{ m}$) existed below the warmer LMVTG.

We adapted a new method to extract multiple LMVTGs objectively from a profile with weak temperature stratification. We changed the threshold of vertical temperature gradient continuously from 2.0 to $0.0^{\circ}\text{C}/100\text{ m}$, at intervals of $0.02^{\circ}\text{C}/100\text{ m}$. Because we also needed to take into account for the colder LMVTG, multiple LMVTGs were extracted objectively from a single profile. Figure 3 shows two typical vertical temperature structures. They were obtained at (a) $35.5^{\circ}\text{ S}, 32.5^{\circ}\text{ E}$ and (b) $35.5^{\circ}\text{ S}, 41.5^{\circ}\text{ E}$. In (a), the warmer LMVTG had a higher vertical temperature gradient than the colder LMVTG, and in (b), the opposite was the case. In (a), the warmer LMVTG was detected with a vertical temperature gradient threshold from 1.56 to $1.32^{\circ}\text{C}/100\text{ m}$, while the colder LMVTG

727

was detected with a vertical temperature gradient threshold from 1.22 to $1.18^{\circ}\text{C}/100\text{ m}$. In (b), the warmer LMVTG was detected with a vertical temperature gradient threshold from 1.20 to $0.86^{\circ}\text{C}/100\text{ m}$, while the colder LMVTG was detected with a vertical temperature gradient threshold from 1.20 to $1.04^{\circ}\text{C}/100\text{ m}$. Therefore, we could detect multiple LMVTGs objectively from a single profile with weak temperature stratification using this method. As a trade-off, we could not examine the thickness of the LMVTG. The thickness of the LMVTG depended on the vertical temperature gradient threshold. Therefore, we focused on the water characteristics of the LMVTG core, which did not depend on thickness.

We extracted water characteristics from a wide area (10 – 50° S , 20 – 120° E) of the Indian Ocean subtropical gyre using this method. Generally, one core was extracted from a single vertical gradient temperature profile in most of the subtropical gyre, while two cores were extracted in the western region of the gyre. The core temperature was higher than 15.5°C between 33 – 38° S and 25 – 50° E (Fig. 4a). An area census of the core temperature and salinity showed two bivariate modes around 8.0 – 14.0°C and 34.3 – 35.3 psu , and around 15.5 – 17.5°C and 35.3 – 35.6 psu (Fig. 4b). The core temperatures higher than 15.5°C were located in the western part of the Indian Ocean subtropical gyre, and the core water characteristics around 16.5°C and 35.5 psu formed a maximum in occurrence frequency on the bivariate classes of temperature and salinity. Therefore, we concluded that IOSTMW existed as a robust structure in the western part of the Indian Ocean subtropical gyre in summer.

According to previous studies, it is reasonable to assume that the other much broader occurrence frequency maximum of core water characteristics around 8.0 – 14.0°C and 34.3 – 35.3 psu is due to two mode waters: mode water centered around 12.0 – 14.0°C and 35.0 – 35.4 psu formed north of the Subtropical Front (STF; 10.0 – 12.0°C and 34.6 – 35.0 psu at 100 dbar ; Orsi et al., 1995), and mode water around 8.0 – 10.0°C and 34.2 – 34.6 psu formed south of the STF, corresponding to Sub-Antarctic Mode Water (SAMW; McCartney, 1977, 1982). A deep mixed layer has been found to form north of the STF in the 60 – 80° E longitude band (Wong, 2005; Aoki et al., 2007). McDonagh et al.

728

(2005) suggested that mode water between 12.0 and 14.0°C at 70° E along the 32° S hydrographic line is subtropical, rather than sub-Antarctic. Because it is difficult to separate these two mode waters objectively using the IOHB climatology, further study of this issue is required.

5 We calculated the averaged IOSTMW water characteristics. All core temperatures higher than 15.5°C were counted. The averaged IOSTMW water characteristics and standard deviations were $16.54 \pm 0.49^\circ\text{C}$, 35.51 ± 0.04 psu, and $26.0 \pm 0.1\sigma_\theta$. According to Bryden et al. (2003), upper thermocline waters (10.0–17.0°C) along the 32° S hydrographic line showed substantial oscillations during 1936–2002. To examine the
10 time period that this averaged IOSTMW water property represented, we investigated the source data used to construct the IOHB. The source data obtained in the region 30–40° S and 20–50° E during January–March are mainly for the period of 1960–2004, with peaks in the 1970s and 1990s. Therefore, we concluded that this averaged water property approximately represented the time period from 1960 to 2004.

15 The water characteristics of the IOSTMW specified above were compared with those described in previous studies. The temperature specified in the present study was about 1°C lower than that mentioned by Olson et al. (1992). Olson et al. (1992) noted the pycnostad with water characteristics of 17.6°C and 35.56 psu and named it the South Indian Subtropical Mode Water as a counterpart to the STMW in the North
20 Atlantic, using the observational data of ARC. The temperature difference between our results and theirs was presumably due to the difference in the analyzed area. The IOSTMW core temperature varied spatially, as indicated in Fig. 2, with higher values in the west. The IOSTMW in Region A (B) had a core temperature of approximately 17.0 (16.5)°C. Our results represent the IOSTMW water characteristics more accurately because we treated the core temperature carefully over a wider region of the
25 Indian Ocean subtropical gyre.

4 Spatial distribution of IOSTMW

In this section, we show the limitations of the LMVTG as a tool for describing the spatial extent of IOSTMW and examine the spatial distribution of the IOSTMW from a different viewpoint. While the North Pacific Central Mode Water (NPCMW; Nakamura, 1996;
5 Suga et al., 1997) formed an LMVTG only in the 35–40° N, 160° E–160° W region, its signature as a lateral minimum of low potential vorticity on the $26.4\sigma_\theta$ isopycnal surface spreads southward widely down to 20° N from the formation area along the gyre flow path (Suga et al., 2004). In the area of weakly stratified temperature structure below the Mode Water, the distribution of the lateral minimum of low potential vorticity sometimes
10 did not correspond to the distribution area of the LMVTG.

Figure 5a shows the distribution of potential vorticity on the $26.1\sigma_\theta$ isopycnal surface, where the IOSTMW water characteristics formed a modal class of temperature and salinity for the area census (Fig. 4b). The lateral minimum of low potential vorticity (less than $300 \times 10^{-12} \text{ m}^{-1} \text{ s}^{-1}$) on the $26.1\sigma_\theta$ isopycnal surface was distributed
15 over the 27–38° S, 25–50° E region. The southern part of this low potential vorticity corresponded quite well to the distribution area of the LMVTG, while the northern part did not. Through careful examination of the northern part, we confirmed that the 15.5–17.5°C layer contained vertical temperature gradients as low as 1.3°C/100 m. This layer did not form the LMVTG because no stronger temperature stratification existed below
20 the 15.5–17.5°C layer. Since the water mass is generally advected on the isopycnal surface, it is reasonable to consider that the whole region of the lateral minimum of potential vorticity is a remnant of the winter mixed layer. Therefore, we concluded that a potential vorticity of less than $300 \times 10^{-12} \text{ m}^{-1} \text{ s}^{-1}$ on the $26.1\sigma_\theta$ isopycnal surface represented the IOSTMW region more accurately.

25 The IOSTMW distribution area was approximated using temperature data with a simple criterion, as described below. Because the IOSTMW core temperature range corresponded to 15.5–17.5°C (Fig. 4b), we could roughly estimate the thickness of the 15.5–17.5°C layer, which was equivalent to a low potential vorticity of $300 \times 10^{-12} \text{ m}^{-1} \text{ s}^{-1}$.

Assuming that the relative vorticity was negligible and the representative vertical salinity stratification was 0.07 psu/100 m in this region, a low potential vorticity less than $300 \times 10^{-12} \text{ m}^{-1} \text{ s}^{-1}$ was equivalent to a 15.5–17.5°C layer greater than 98.9 m, according to Eq. (1):

$$\rho v \approx \frac{f}{\rho} \frac{\partial \rho}{\partial z} \approx \frac{f}{\rho} \left(\alpha \frac{dT}{dz} + \beta \frac{dS}{dz} \right) \quad (1)$$

in which the thermal expansion coefficient α and haline contraction coefficient β were calculated using the averaged IOSTMW water characteristics, and the Coriolis parameter f at 30° S was used. The area where the 15.5–17.5°C layer thickness was greater than 100 m corresponded fairly closely to a distribution area of low potential vorticity less than $300 \times 10^{-12} \text{ m}^{-1} \text{ s}^{-1}$ on the $26.1 \sigma_\theta$ isopycnal surface (Fig. 5b). We thus suggest that the spatial distribution of the 15.5–17.5°C layer greater than 100 m represented the distribution area of the IOSTMW.

It is interesting to note the geographical coincidence between the IOSTMW distribution area and the South West Indian Ocean sub-gyre (Lutjeharms, 2006). This anticyclonic gyre may correspond to weaker temperature/density stratification in the center of the sub-gyre. This is a favorable condition for deeper winter mixed layer formation. The IOSTMW formation area should correspond to a weaker temperature/density stratification area under stronger winter cooling.

5 Conclusions

We have presented a basic description (water characteristics and spatial distribution) of the IOSTMW using an isopycnally averaged three-dimensional hydrographic dataset. We found that we could not detect the whole IOSTMW as an LMVTG using any single vertical temperature gradient threshold because a weak temperature stratification existed below the IOSTMW. By changing the threshold of vertical temperature gradient continuously, we confirmed that the LMVTG was located in the western part of the

731

Indian Ocean subtropical gyre as a substantial water mass, and that its core water characteristics formed a mode on the bivariate classes of temperature and salinity for the area census. We thus concluded that the IOSTMW existed as a robust structure in this region in summer. The averaged water characteristics of the IOSTMW during approximately 1960–2004 were $16.54 \pm 0.49^\circ\text{C}$, 35.51 ± 0.04 psu and $26.0 \pm 0.1 \sigma_\theta$. The temperature of the IOSTMW was about 1°C lower than that recognized in previous studies. A lateral minimum of low potential vorticity (less than $300 \times 10^{-12} \text{ m}^{-1} \text{ s}^{-1}$) associated with the IOSTMW was distributed in the 25–50° E, 27–38° S region on the $26.1 \sigma_\theta$ isopycnal surface, where the IOSTMW water characteristics formed a mode on the bivariate classes of temperature and salinity. Although this area was wider than the LMVTG distribution area, it represents the IOSTMW distribution area more accurately. The IOSTMW distribution area was easily described as the area where the 15.5–17.5°C layer had thickness greater than 100 m.

Acknowledgement. We wish to express our sincere thanks to members of the Physical Oceanography Group at Tohoku University for fruitful discussions. This study was performed as a part of the 21st Century Center-of-Excellence (COE) Program “Advanced Science and Technology Center for Dynamic Earth (E-ASTEC)” at Tohoku University. The English in this document has been checked by at least two professional editors, both native speakers of English. For a certificate, see: <http://www.textcheck.com/cgi-bin/certificate.cgi?id=Jwg2uM>

20 References

- Akima, H.: A new method of interpolation and smooth curve fitting based on local procedures, J. Assoc. Comput. Math., 17, 589–602, 1970.
- Aoki, S., Hariyama, M., Mitsudera, H., Sasaki, H., and Sasai, Y.: Formation regions of Subantarctic Mode Water detected by OFES and Argo profiling floats, Geophys. Res. Lett., 34, L10606, doi:10.1029/12007GL029828, 2007.
- Boyer, T. P., Stephens, C., Antonov, J. I., Conkright, M. E., Locarnini, R. A., O’Brien, T. D., and Garcia, H. E.: World Ocean Atlas 2001, Vol. 2, Salinity, NOAA Atlas NESDIS 50, CD-ROM., 2002.

732

- Bryden, H. L., McDonagh, E. L., and King, B. A.: Changes in ocean water mass properties: Oscillations or trends? *Science*, 300, 2086–2088, 2003.
- Fine, R. A.: Circulation of Antarctic Intermediate Water in the South Indian-Ocean, *Deep-Sea Res.*, 40, 2021–2042, 1993.
- 5 Gordon, A. L., Lutjeharms, J. R. E., and Grundlingh, M. L.: Stratification and Circulation at the Agulhas Retroflexion, *Deep-Sea Res.*, 34, 565–599, 1987.
- Hanawa, K. and Talley, L. D.: *Mode Waters, Ocean Circulation and Climate: Observing and Modelling the Global Ocean*, edited by: Siedler, G., Church, J., and Gould, J., Academic Press, London, 373–386, 2001.
- 10 Hanawa, K. and Sugimoto, S.: “Reemergence” areas of winter sea surface temperature anomalies in the world’s oceans, *Geophys. Res. Lett.*, 31, L10303, doi:10.1029/12004GL01904, 2004.
- Kobayashi, T. and Suga, T.: The Indian Ocean HydroBase: A high-quality climatological dataset for the Indian Ocean, *Prog. Oceanogr.*, 68, 75–114, 2006.
- 15 Lutjeharms, J. R. E.: *The Agulhas Current*, Springer, Berlin, p. 329, 2006.
- Marshall, J. C., Nurser, A. J. G., and Williams, R. G.: Inferring the Subduction Rate and Period over the North-Atlantic, *J. Phys. Oceanogr.*, 23, 1315–1329, 1993.
- Masuzawa, J.: Subtropical mode water, *Deep-Sea Res.*, 16, 453–472, 1969.
- McCartney, M. S.: Subantarctic Mode Water, in: *A Voyage of Discovery: George Deacon 70th Anniversary Volume*, edited by: Angel, M., Pergamon Press, Oxford, 103–199, 1977.
- 20 McCartney, M. S.: The subtropical recirculation of mode waters, *J. Mar. Res.*, 40, 427–464, 1982.
- McDonagh, E. L., Bryden, H. L., King, B. A., Sanders, R. J., Cunningham, S. A., and Marsh, R.: Decadal changes in the south Indian Ocean thermocline, *J. Climate*, 18, 1575–1590, 2005.
- 25 Nakamura, H.: A pycnostad on the bottom of the ventilated portion in the central subtropical North Pacific: Its distribution and formation, *J. Oceanogr.*, 52, 172–188, 1996.
- Olson, D. B., Fine, R. A., and Gordon, A. L.: Convective modification of water masses in the Agulhas? *Deep-Sea Res.*, 39, S163–S181, 1992.
- Orsi, A. H., Whitworth, T., and Nowlin, W. D.: On the meridional extent and fronts of the Antarctic Circumpolar current, *Deep-Sea Res.*, 42, 641–673, 1995.
- 30 Stephens, C., Antonov, J. I., Boyer, T. P., Conkright, M. E., Locarnini, R. A., O’Brien, T. D., and Garcia, H. E.: *World Ocean Atlas 2001, Vol. 1, Temperature*, NOAA Atlas NESDIS 49, CD-ROM, 2002.

733

- Suga, T., Takei, Y., and Hanawa, K.: Thermocline distribution in the North Pacific subtropical gyre: the central mode waters and the subtropical mode water, *J. Phys. Oceanogr.*, 27, 140–152, 1997.
- Suga, T., Motoki, K., Aoki, Y., and Macdonald, A. M.: The North Pacific climatology of winter mixed layer and mode waters, *J. Phys. Oceanogr.*, 34, 3–22, 2004.
- 5 Toole, J. M. and Warren, B. A.: A hydrographic section across the south Indian-Ocean, *Deep-Sea Res.*, 40, 1973–2019, 1993.
- Wong, A. P. S.: Subantarctic mode water and antarctic intermediate water in the South Indian ocean based on profiling float data 2000–2004, *J. Mar. Res.*, 63, 789–812, 2005.

734

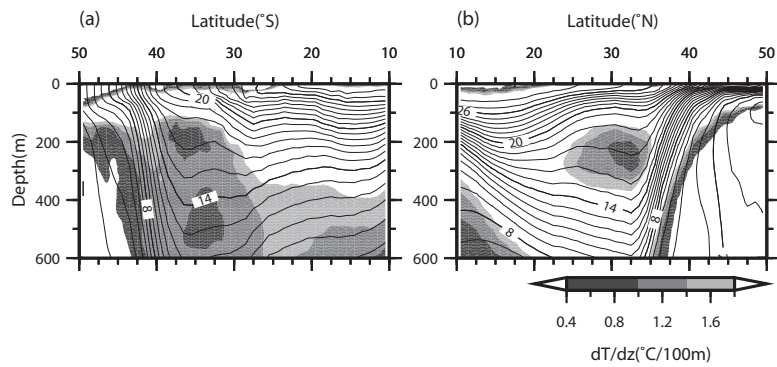


Fig. 1. Meridional temperature sections of the western part of the subtropical gyre in the **(a)** Indian Ocean (42.5° E) and **(b)** North Pacific (145.5° E). The contours show the temperature (°C), and the gray shading shows the vertical temperature gradient (°C/100 m).

735

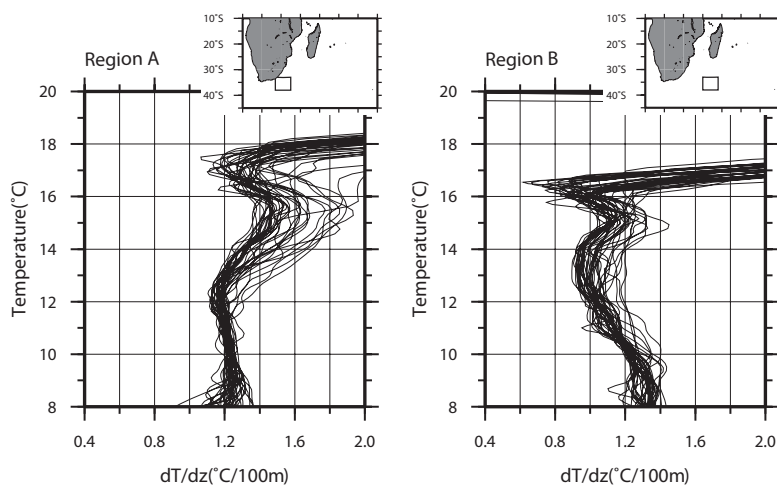


Fig. 2. Relationship between the vertical temperature gradient (°C/100 m) and temperature (°C) in two selected sub-regions. The map shows the locations of Region A (33–38° S and 27–35° E) and Region B (33–38° S and 40–48° E).

736

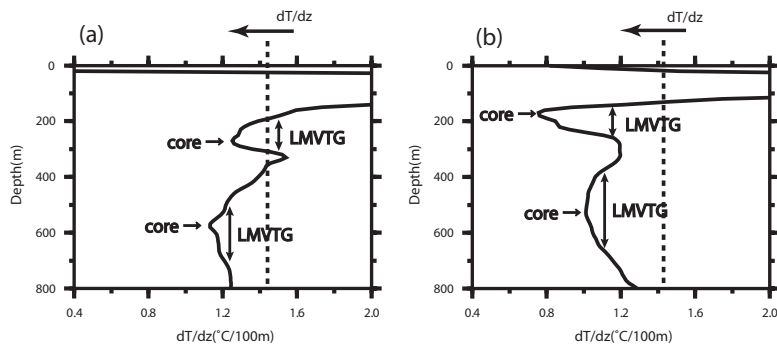


Fig. 3. Schematic of the method for detecting multiple LMVTGs from a single profile. Two typical conceivable vertical temperature gradient structures ($^{\circ}\text{C}/100\text{ m}$) are shown: **(a)** 35.5° S , 32.5° E and **(b)** 35.5° S , 41.5° E . The dotted line shows the threshold of vertical temperature gradient, which was varied continuously from 2.0 to $0.0^{\circ}\text{C}/100\text{ m}$ in $0.02^{\circ}\text{C}/100\text{ m}$ intervals.

737

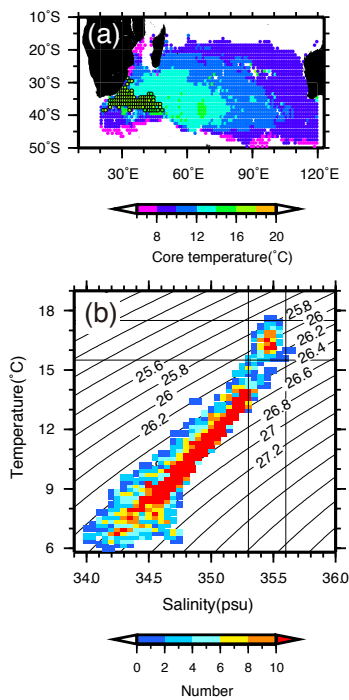


Fig. 4. **(a)** Spatial distribution of the core temperature and **(b)** occurrence frequency of core water characteristics on the bivariate classes of temperature and salinity in the $10\text{--}50^{\circ}\text{ S}$, $20\text{--}120^{\circ}\text{ E}$ region. When two cores were detected at a certain grid point, the higher core temperature was plotted on the spatial distribution of core temperature, and both core water characteristics were counted to calculate the occurrence frequency. In **(a)**, core temperatures higher than 15.5°C are circled by a solid line.

738

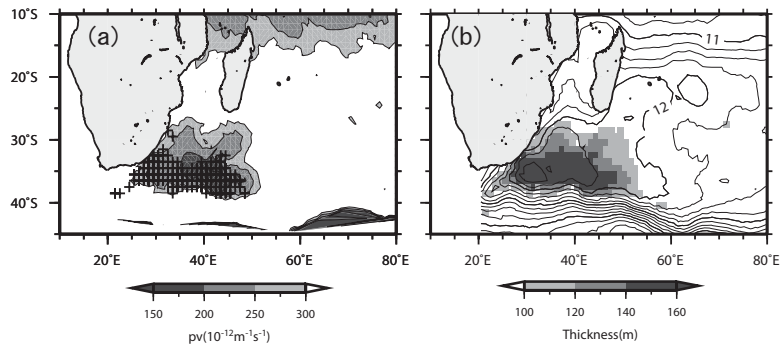


Fig. 5. (a) Distribution of potential vorticity ($10^{-12} \text{ m}^{-1} \text{ s}^{-1}$) on the $26.1\sigma_\theta$ isopycnal surface. The crosses represent all LMVTG positions with a core temperature higher than 15.5°C , which were detected by changing the threshold of vertical temperature gradient continuously from $2.0^\circ\text{C}/100 \text{ m}$ to $0.0^\circ\text{C}/100 \text{ m}$ at $0.02^\circ\text{C}/100 \text{ m}$ intervals. (b) The spatial distribution of the thickness of the $15.5\text{--}17.5^\circ\text{C}$ layer greater than 100 m is superimposed on the dynamic height ($\text{m}^2 \text{ s}^{-2}$) at 200 m .